**Title**
Mode-2 internal solitary wave velocity fields and the effects of shear

**Permalink**
https://escholarship.org/uc/item/9ww0h59m

**Journal**
International Symposium on Stratified Flows, 1(1)

**Authors**
Kalumuck, Kenneth
Brandt, Alan

**Publication Date**
2016-09-01

# Mode-2 Internal Solitary Wave Velocity Fields and the Effects of Shear

Kenneth M. Kalumuck and Alan Brandt

Johns Hopkins University Applied Physics Laboratory
kenneth.kalumuck@jhuapl.edu

**Abstract**

Mode-2 ISW are known to transport mass and to contain regions of recirculating flow. To better understand the characteristics of mode-2 Internal Solitary Waves (ISW) laboratory experiments were performed in a two-layer counter-flow stratified shear tunnel with a thin pycnocline. Detailed velocity field measurements using PIV were made of the evolving flow within and around the ISW under both quiescent ambient and vertical shear flow conditions. When converted to a reference frame moving with the ISW, the observed flow fields readily show a combination of recirculating zones and solid body type motion (zero velocity relative to the wave speed). In addition regions of entrainment/detrainment and small structure formation within the ISW bulge were observed. The effect of shear is to suppress the ISW in regions in which it propagates against the local ambient flow so that the wave is present primarily on only one side of the density/shear profile.

## 1 Introduction

There have been an increasing number of observations of mode-2 Internal Solitary Waves (ISW) in the coastal ocean (e.g., Ramp et al. 2012; Shroyer et al. 2010; Guo & Chen 2014; Yang et al. 2009). Large amplitude mode-2 solitary waves have unique properties including regions of internal recirculation that enable mass transport over large distances. Such waves, which can have amplitudes of many tens of meters, can affect upper ocean mixing, the distribution of biological and chemical constituents, contaminant transport, the propagation and scattering of acoustic signals (Orr 2012) and the maneuvering and control of submerged bodies. Recently, Brandt & Shipley (2013, 2014) made the first quantitative measurements of mass transport by mode-2 ISW propagating on a thin pycnocline in the stratified shear channel shown in fig 1. This work identified three classes of mode-2 ISW based on their amplitude. It also highlighted the importance of the recirculation region of the ISW, which is responsible for the transport of mass and undergoes different behaviors (including entrainment, detrainment, mixing and instabilities) at different wave amplitudes. The effects of shear on ISW propagation and mass transport are of significant interest since vertical shear is ubiquitous in the coastal ocean. This paper presents results of PIV measurements of mode-2 ISW flow fields focusing on the recirculating cells for mass transport in the presence of shear conducted in the same facility used in Brandt & Shipley (2013, 2014).

## 2 Experimental Setup

Laboratory studies were conducted in the stratified shear channel shown in fig. 1 (20.3 x 7.6 x 600 cm) designed to produce a nominally 2D flow. Two fluid layers of equal depth and different densities were employed – a fresh water layer above a salt water (typically 50 ppt). A thin interface layer formed a transition in density between the two fluids. The two fluid layers were mixed by an oscillating plate at one end thereby forming a train of mode-2 ISW

1

propagating along the interface. (In some cases a mixing box was used to contain the mixed fluid and then removed to release the fluid.) The general nature of the evolving flow can be seen in the photo in fig. 1 which shows both the leading and following mode-2 ISW. Here, the denser fluid is dyed blue, the fresh water is clear, and the mixed fluid is dyed red to visualize the propagating mode-2 ISW and its mass transport. Brandt & Shipley (2014) provides a fuller description of the tank and measurements of ISW characteristics and mass transport. Vertical shear was created by establishing a counter flow such that the top and bottom layers were moving at nominally the same speeds in opposite directions and that the centers of the vertical density and shear profiles coincided.
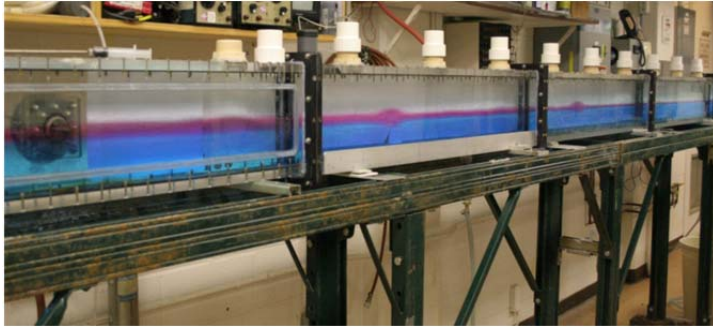


Figure 1: Mode-2 ISW in stratified shear channel propagating on interface between upper clear fresh water & bottom blue salt water layers. The ISW-transported mass is shown in red.
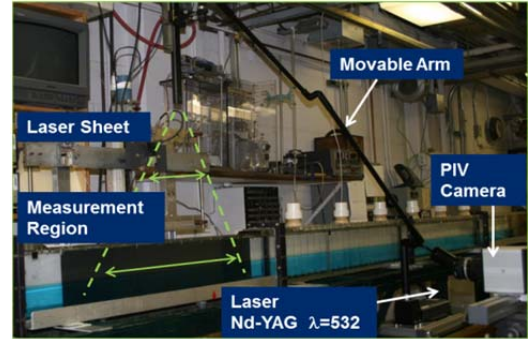


Figure 2: PIV setup in shear channel of fig 1.

Velocity field measurements were made with the PIV system setup shown in fig. 2 using a vertical Nd-YAG laser sheet along the span-wise center of the tank producing a field of view approximately 35 cm in stream-wise extent and spanning the channel depth. To facilitate the PIV measurements, the top was removed from a section of the channel. Both the mixed fluid region (transported with the ISW) and the imaged channel section were seeded. Velocity fields were imaged at 10 Hz and processed using DaVIS software to achieve a spatial resolution of ~ 1.3 mm. In several cases, a smaller field of view was employed to obtain a spatial resolution of 0.6 mm. Given that the observed wave speeds were ~ 2-6 cm/s with wavelengths ~ 10 cm, this provides good temporal and spatial resolution. Imaging of both the first and trailing waves resulted in approximately 200-300 images for each run.

Prior to each run the density profile was measured with a vertically traversing conductivity/temperature probe. The profiles were fit well the commonly used relation

$$\rho(z) = \rho_0 \left[ 1 - \frac{\Delta\rho}{2\,\rho_0} tanh\left(\frac{z}{h}\right)\right].$$

Here, ρ is the density as a function of depth z measured from the interface, Δρ the difference in layer densities, $\rho_0$ a reference (average) density, and h the characteristic layer thickness. Typically, h ~ 0.5-1 cm (5-10% of each layer thickness). For cases with shear there was greater asymmetry in the density profiles with the bottom layer interface thickness being larger than that of the top. Shear profiles were measured by tracking the temporal evolution of an injected of

vertical dye line. Measured vertical shears were ~ 1 – 2.5 s$^{-1}$ with shear layer half thicknesses of ~ 2-4 cm.

Wave speeds were measured by tracking the advancement in time of the observed mode-2 "bulges". The wave speed of a long infinitesimal interfacial mode-2 wave is given by

$$c_0 = \frac{1}{2} \left( \frac{gh\Delta\rho}{\rho_0} \right)^{\frac{1}{2}}.$$

The measured speeds, c, of the nonlinear mode-2 ISW reported here are ~ 2c$_o$ and larger

## 3  Results

An example result is presented in fig. 3, which shows the velocity and vorticity fields measured with PIV at one location at a single instant of time for a mode-2 ISW in the absence of shear. The black horizontal line marks the center of the measured density interface, here at a depth of 11 cm. A strong recirculation region can be seen that includes significant vorticity along the top and bottom edges of the bulge. Of note are the top to bottom asymmetry in the velocity/vorticity fields, the weaker counter-rotating flow at the lower aft end of the bulge, and the weaker recirculation (indicating mode-2) in a trailing wave.  The strong vorticity at the top aft end of the first bulge likely contributes to the roll-up instabilities in this region observed by Brandt & Shipley (2014). The lack of such vorticity at the lower aft end of the bulge could explain why these instabilities were observed primarily on the upper aft of the bulge and not the lower.
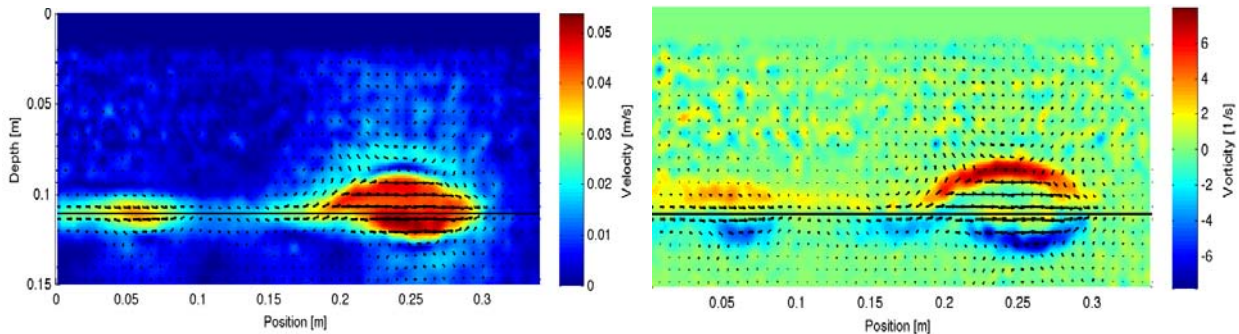


Figure 3: Instantaneous flow fields measured with PIV for leading and first following mode-2 ISW propagating from left to right. Shown are contours of velocity magnitude (left) and span-wise vorticity (right) overlaid with velocity vectors (both).

To better understand the mechanisms at work, it is instructive to look in more detail at the velocity fields both in the laboratory frame of reference and in a frame of reference moving with the ISW. The latter was obtained for each ISW by subtracting its speed, c, from the stream-wise velocity. The laboratory reference frame is useful for examining the areas of entrainment/detrainment and instability. Use of the ISW reference frame enables detailed examination of the flow field within the ISW, which, as is seen below, can be of much smaller magnitude than its advance (wave) speed.

Figs. 4-6 present velocity field results in both reference frames for three cases of varying vertical shear: 0, 1.2, 2.4 s$^{-1}$. For each case, the upper figure shows the detailed velocity vector

field in the laboratory reference frame overlaid on the resulting vorticity. The lower figure presents a portion of the velocity field within the ISW (denoted by a pink colored box) that has been expanded and converted to the individual ISW frame of reference.
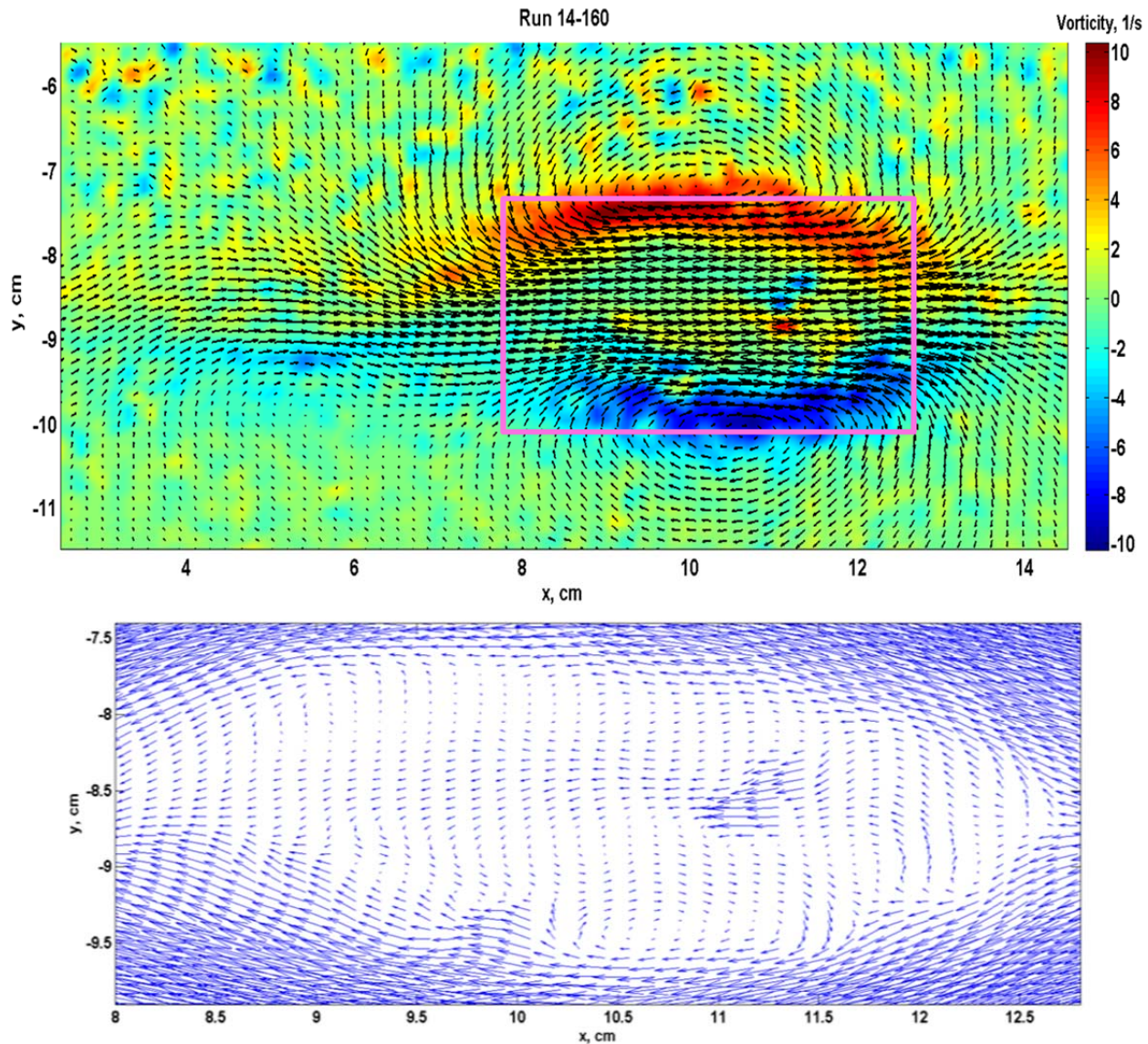


Figure 4: Instantaneous flow fields measured with PIV for mode-2 ISW propagating from left to right in the absence of shear ( c=4 cm/s, $c/c_o$=1.8). Top: velocity vectors in the laboratory frame of reference overlaid on vorticity contours. Bottom: velocity vectors in the ISW frame of reference over the region outlined by the box in the upper figure.

In the no-shear case, fig. 4, strong circulating flows can be observed in the top figure on both the top and bottom of the bulge with the center of the bottom circulatory flow located somewhat forward of that of the top circulatory flow. The inner edges of the circulatory regions are accompanied by strong regions of span-wise vorticity as the velocities rapidly achieve an approximately stream-wise direction. Also observable are weaker regions of opposite sign vorticity near the center of the bulge. Similar opposite-signed vorticity regions have recently

4

been predicted numerically by Deepwell & Stastna (2016). Entrainment at the rear of the bulge can be observed as can the formation of a weaker circulating region in the wake behind the bulge.

The lower image of fig. 4, in the ISW reference frame, clearly shows an elongated inner recirculation region within the bulge and surrounded by a larger outer cell that appears to flow around the bulge but in reality is moving with the bulge (as can be seen from the laboratory reference frame), but at an advance seed a bit less than that of the central region. It is this behavior that is responsible for the inner and outer regions of oppositely signed vorticity. Penetration into the lower aft of the bulge is also observed producing an asymmetry.
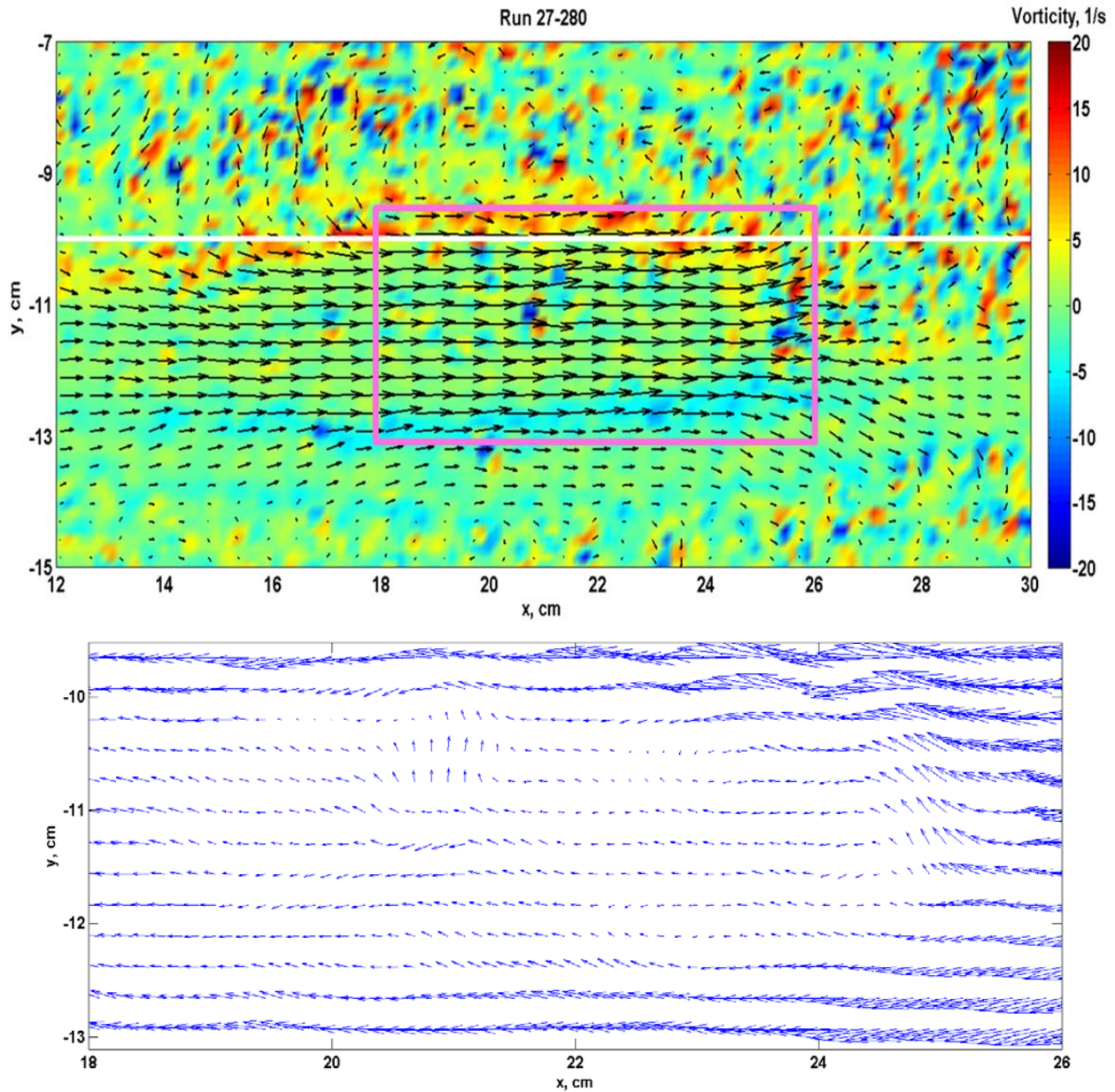


Figure 5: Effect of a vertical shear of ~ 1.2/s (c=4.9 cm/s, $c/c_o$=1.9). White line in upper image denotes center of density interface. Same quantities presented as in fig. 4.

Introduction of shear affects both the ISW bulk behavior and the details of its velocity field as can be seen in figs. 5 and 6 which represent increasing amounts of vertical shear. The shear flow is such that the flow in the lower layer is from left to right – in the direction of ISW propagation, while that in the upper layer is from right to left, against the direction of ISW propagation. In both cases the wave is suppressed in the upper layer while propagating within the lower layer. This can be seen by referring to the white horizontal line in each upper image that demarks the center of each density profile.
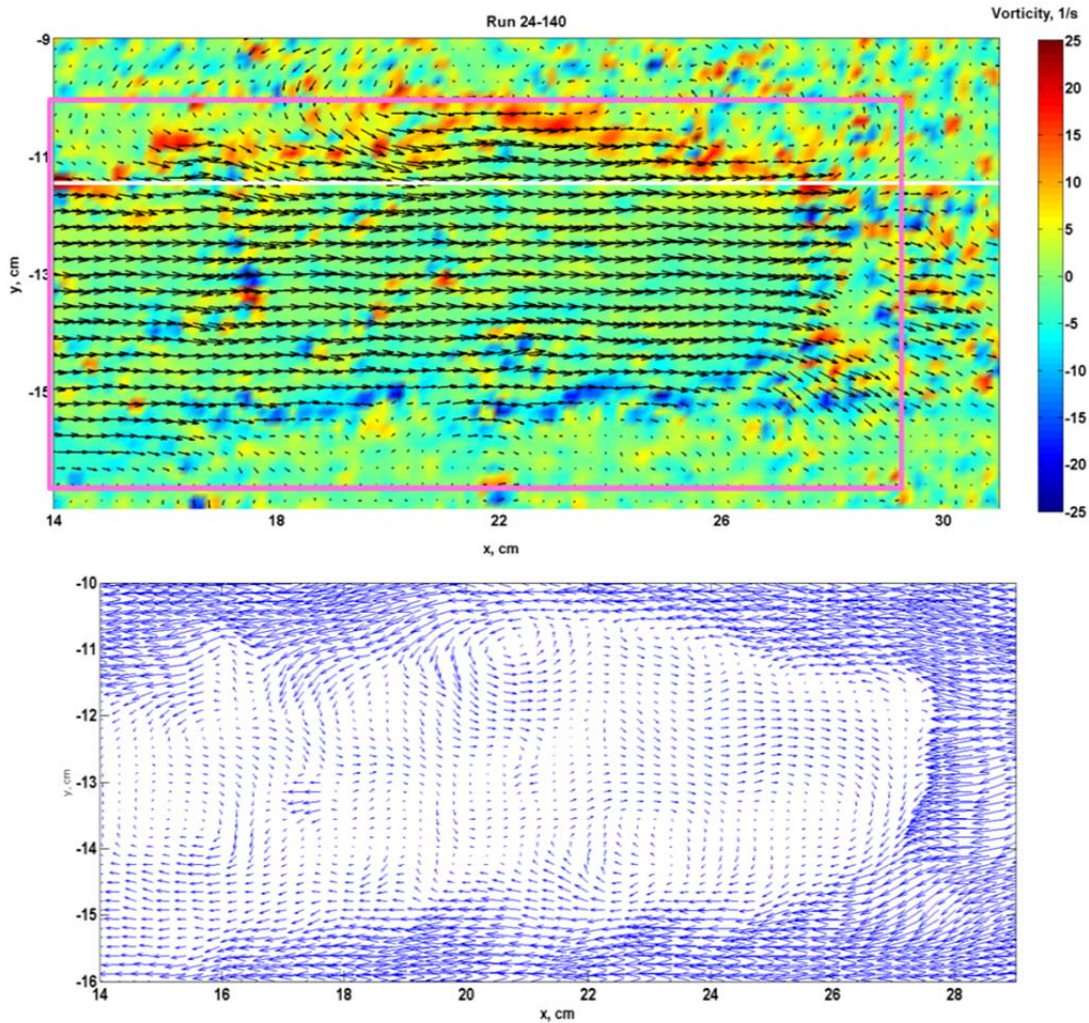


Figure 6: Effect of a vertical shear of ~ 2.4/s (c=5.7 cm/s, $c/c_o$=1.7). White line in upper image denotes center of density interface. Same quantities presented as in figs. 4 & 5.

In both cases, the regions of strong coherent vorticity of the bulges have been disrupted and replaced with much more localized patches of vorticity. This is true for both the outer shell of vorticity and the inner region of opposite signed vorticity indicating potentially the onset of unsteady and possibly unstable or turbulent flow, particularly at finer scales. At scales of the order of the bulge dimensions, there still remain outer layers of vorticity of the same sign as the no-shear case, but they are thinner and irregular. Entrainment at the aft of the bulge on both its top and bottom are still apparent, but the flow lines are more elongated. At the higher shear (fig.

6), the surface denoted by both the vorticiy and velocity vectors can be seen to be particularly irregular with some undulation suggesting the beginning of shear instabilities, particularly on the upper aft boundary.

Examination of the interiors of the bulges in the shear cases in the ISW reference frames shows a general increase in disorder and a reduction in scale of the recirculation zones with increasing shear. The flow field of the lower image of fig 5, the lower shear case, exhibits almost wave-like behavior. However, it may also be the incipient splitting of the elongated inner recirculation cell observed without shear (fig. 4) into separate cells aligned in the stream-wise direction one in front of the other. This possibility is supported by the velocity vectors in the higher shear case of fig. 6. These vectors indicate that the ISW consists of several different recirculating regions whose characteristic sizes in the stream-wise and vertical directions are much more comparable than those of the elongated region in the absence of shear (fig. 4). Strong cells can be seen in the top middle, lower middle, and front as well as several in the rear. Also apparent is the very irregular outer envelope of the main flow passing around these recirculating regions and likely penetrating into the bulge (e.g., at the top at x ~ 17 cm in fig. 6) creating mixing, entrainment, and likely turbulence or instabilities.  Likely detrainment loss of fluid from the bulge is indicated by the vectors on the lower aft of the bulge.

It should be remembered that the flow fields in the ISW frame of reference are superposed on the propagation velocities of the ISW creating a phenomenon that both transports mass but also gradually entrains fluid while leaving other fluid behind thus enabling mixing and spreading of mass over large distances.

## 4  Conclusions

PIV measurements of laboratory generated large amplitude mode-2 ISW have revealed the prevalence and complexity of internal recirculating regions that enable transport of mass by these waves. The measured velocity fields and span-wise vorticity provide an explanation for the oft-observed (by flow visualization) top/bottom asymmetry of these waves. In the absence of shear, the waves reported were found to have an outer region of strong span-wise vorticity generated by the advancing bulge against the background fluid with an internal recirculating region of opposite vorticity. Regions of entrainment, detrainment, and potential incipient instability are observed. The presence of shear results in a suppression of the wave propagation in a direction against the current while the wave continues to propagate in regions moving with the current. Shear also affects both the outer envelope of the bulge and its interior flow creating more irregular, less organized flow patches and smaller-scale recirculation zones within the bulge indicating the potential for onset of instabilities and turbulence.

**References**.

Brandt, A. (2007). Evolution of mode-2 solitary internal waves in a stratified shear flow. *Proc. 6th International Symposium on Environmental Hydraulics (ISEH V)*, Tempe, Arizona.

Brandt, A. & Shipley, K. (2013). Mass transport by large and very-large amplitude mode-2 internal solitary waves: experimental observations. Invited to *3rd DNVA-RSE Norway-Scotland Waves Symp.*, Oslo, Norway.

Brandt, A. & Shipley, K. (2014). Laboratory experiments on mass transport by large amplitude Mode-2 internal solitary waves. *Phys. Fluids,* 26(4), 046601.

Deepwell, D., & Stastna, M. (2016). Mass transport by mode-2 internal solitary-like waves. *Physics of Fluids*, 28(5): 056606.

Guo, C. & Chen, X. (2014). A review of internal solitary wave dynamics in the northern South China Sea, *Progress in Oceanography* 121: 7–23.

Orr, M.H. (2012). Mode-2 internal wave generation and propagation - impact on acoustic signal properties. 164th Mtg. ASA, Sept. *J. Acoust. Soc. Am.,* 132: No. 3, Pt. 2: 1897.

Ramp, S., Yang, Y., Reeder, D., Bahr, F. (2012). Observations of a mode-2 nonlinear internal wave on the northern Heng-Chun ridge south of Taiwan. *JGR,* 117, C03043.

Shroyer, E.L., Moum, J.N, & Nash, J.D. (2010) Mode-2 waves on the continental shelf: Ephemeral components of the nonlinear internal wave field. *JGR,* 115, C03022.

Yang, Y., Fang, Y., Chang, M., Ramp, S., Hao, C., & Tang, T. (2009). Observations of 2nd baroclinic mode internal solitary waves on the continental slope of the northern South China Sea. *JGR,* 114, C10003.